


Article

Adsorption of Heavy Metals and Biocides from Building Runoff onto Granular Activated Carbon—The Influence of Different Fractions of Dissolved Organic Matter

Panfeng Zhu, Ignacio Sottorff, Tong Zhang and Brigitte Helmreich * 

Chair of Urban Water Systems Engineering, TUM School of Engineering and Design, Technical University of Munich, Am Coulombwall 3, 85748 Garching, Germany; panfeng.zhu@tum.de (P.Z.); i.sottorff@tum.de (I.S.); t.zhang@tum.de (T.Z.)

* Correspondence: b.helmreich@tum.de; Tel.: +49-89-289-13719

Abstract: Building runoff presents a good opportunity for water reuse in urban infrastructures; however, it is often polluted by biocides and heavy metals. In order to mitigate the pollution and improve water quality, we analysed the adsorption of heavy metals and biocides onto granular activated carbon (GAC) and investigated the influence of dissolved organic matter (DOM) fractions (>100 kDa, 10–30 kDa, and 3–10 kDa). In addition to our experimental work, we also studied the adsorption process by applying the Langmuir and Freundlich models. The results showed that $\geq 50\%$ of DOM was adsorbed at low concentrations (5 mgC/L). We also observed that DOM at a small molecular size exhibits improved adsorption. The adsorption capacity estimated by the Langmuir equation for Cu^{2+} and Zn^{2+} in the absence of DOM influence was 157 and 85.7 $\mu\text{mol/g}$, respectively. The presence of DOM at 5 mgC/L improved the adsorption of Cu^{2+} . Zn^{2+} adsorption was less sensitive to the presence of DOM than Cu^{2+} . Interestingly, without the influence of DOM, diuron-related compounds have a higher affinity toward GAC than terbutryn-related compounds. DOM affected the adsorption of diuron slightly. For terbutryn, the adsorption was enhanced, whereas mecoprop-p exhibited a strong competition with DOM. The presence of Cu^{2+} and Zn^{2+} presented a similar effect on the adsorption of biocides like DOM. Overall, GAC is an ideal adsorbent material for use in retaining building runoff pollutants.

Keywords: building runoff; biocides; DOM; heavy-metals; GAC; transformation products; water reuse



Citation: Zhu, P.; Sottorff, I.; Zhang, T.; Helmreich, B. Adsorption of Heavy Metals and Biocides from Building Runoff onto Granular Activated Carbon—The Influence of Different Fractions of Dissolved Organic Matter. *Water* **2023**, *15*, 2099. <https://doi.org/10.3390/w15112099>

Academic Editor: Laura Bulgariu

Received: 12 May 2023

Revised: 30 May 2023

Accepted: 31 May 2023

Published: 1 June 2023



Copyright: © 2023 by the authors. Licensee MDPI, Basel, Switzerland. This article is an open access article distributed under the terms and conditions of the Creative Commons Attribution (CC BY) license (<https://creativecommons.org/licenses/by/4.0/>).

1. Introduction

Runoff from buildings (roof and façade runoff) is a non-negligible part of urban stormwater runoff. It can be considered a water supply source for the urban water cycle [1,2]. A basic requirement for the utilization of runoff water is its good quality. However, building runoff presents drawbacks, including heavy metal and biocide pollution. The release of heavy metals comes from metal roofs, gutters, chimneys, and dormers as a result of corrosion [3]. The main players are Cu^{2+} and Zn^{2+} . The reported concentrations of these two heavy metals can be up to 4.9 mg/L for Cu^{2+} [4] and 32 mg/L for Zn^{2+} [5] in copper and zinc roof runoff, respectively. It has been observed that more than 80% of copper and zinc were in the dissolved form as Cu^{2+} and Zn^{2+} ions [5]. This finding indicates that the majority of copper and zinc in metal roof runoff is bioavailable. A high proportion (>90%) of dissolved heavy metals in metal roof runoff was also reported by Müller et al., 2019 [6]. This untreated metal roof runoff poses a huge threat to surface water quality and even to groundwater. The appropriate removal of heavy metals is required before the runoff water enters the environment and/or the runoff is reused.

Additionally found in building runoff are biocides, which leach from the building façades during rain events [7–10] through the water-filled pores [7,10]. In general, biocides

are described as substances used to control unwanted organisms that are harmful to human or animal health or to the environment, or that cause damage to human activities. Some well-known biocides found in construction materials include isoproturon, diuron, carbendazim, terbutryn, and others. [7,10–12]. The concentration of these chemicals in façade runoff is high in the early lifetime of the painting material and decreases with increasing exposure time. Previous research has shown that the diuron and terbutryn concentration in runoff can reach around 20 mg/L and 2 mg/L, separately, upon initial contact of the façade with rainwater [13]. In a case study with an exposure time of 1.5–3 years, it was discovered that diuron and terbutryn in the façade runoff still yielded concentrations around 900 µg/L and 20 µg/L, respectively [12].

Also noteworthy is the biocide mecoprop-p, which is used on roofing materials. This biocide is added to bitumen roof sealing membranes in the form of esters in order to protect them against root penetration on flat green roofs [14]. The amount of mecoprop-p emitted in runoff is not always constant and largely depends on the rain event [8,15,16]. In a given roof, a higher emission level is initially observed after the new installation [16], followed by a decrease in the washout concentration and load after several years [15].

Considering the damaging effects of biocides on the ecosystem (e.g., the inhibition of soil microbial activity [17]), their penetration through sand/clayey soil [18], and the unreliable retention by urban stormwater infiltration systems [19], an appropriate mitigation method for the biocides from runoff is needed to prevent the contamination of soil, aquatic environment, and groundwater.

In this context, a granular activated carbon (GAC)-based decentralized on-site runoff treatment is a promising option in the mitigation of building runoff pollution because such a system has the advantages of high efficiency, cost-effective, and flexibility in construction. As a porous material with a large surface ratio, GAC has been previously applied in stormwater pollution elimination [20–23] and water quality assurance [24–27].

Research on building runoff has thus far mainly focused on the field pollution survey, pollutant leaching simulations, and modelling. Less effort has been made regarding the aspect of decentralized on-site building runoff treatments or to the aspect that both heavy metals and biocides are present in the runoff, not just one or the other. Moreover, there is also the possibility of an additional influence from naturally occurring dissolved organic matter (DOM) on the sorption behaviour onto GAC, which could lead to a reduction in sorption capacity. The utilization of building runoff has been limited by insufficient study of above aspects; therefore, our study aims to fulfil the knowledge gaps and remove the barrier in building runoff reuse.

In this research, we evaluated the adsorption capacity of pollutants in building runoff toward GAC, with a particular focus on biocides, biocide transformation products (BTPs), heavy metals, and DOM occurring both alone and simultaneously. The present study consists of three main parts. Firstly, the investigation of the adsorption of each pollutant onto GAC at different concentrations. Secondly, the quantitative description of adsorption processes via the Langmuir and Freundlich models. Thirdly, studying the influence of the presence of DOM on the adsorption of heavy metals and biocides. We further study the influence of heavy metals on the adsorption of biocides without DOM. The results from this research will contribute to the development of new strategies for the treatment of building runoff, thus achieving pollution source control and the protection of urban environment.

2. Materials and Methods

2.1. DOM Fractionation via Centrifugation

DOM was obtained from Carl Roth® (Karlsruhe, Germany) in the form of humic acid sodium salt, which was previously used in a study focused on proving the interaction between biocides and DOM via fluorescence changes [28]. The fractionation of DOM was performed using centrifugation according to their differences in molecular weight. Before the centrifugal fractionation, DOM stock solution (around 2 g/L) was first particle-cleaned via centrifugation (Centrifuge 5804R; Eppendorf, Berzdorf, Germany) twice in 50 mL tube

at $5000\times g$ for 10 min. The supernatant was then filtered through a $0.45\ \mu\text{m}$ nitrocellulose membrane (Sartorius[®], Goettingen, Germany) to remove the remaining particles and to avoid clogging the membranes for further fractionation. The fractionation membranes used (from Pall[®], Ann Arbor, MI, USA and Sartorius[®]) had molecular weight cut offs at 100 kDa, 30 kDa, 10 kDa, and 3 kDa. A sequential centrifugation process was accordingly adopted, where the centrifugation speed was $6000\times g$, the time of centrifugation ranged from 4 to 60 min, which increased with decreasing DOM fraction size. At the end, the DOM fractions $> 100\ \text{kDa}$, 30–100 kDa, 10–30 kDa, 3–10 kDa, and $<3\ \text{kDa}$ were obtained and stored in glass bottles at $4\ ^\circ\text{C}$. After an appropriate dilution, the concentrations of dissolved organic carbon (DOC) in these five DOM fractions were measured using a total organic carbon (TOC) analyser (vario, Elementar[®], Langensfeld, Germany).

2.2. Granular Activated Carbon Preparation

The GAC used in this study was Cyclecarb 301 (Chemviron[®], Hattersheim, Germany). In order to avoid the influence from large GAC particles and maintain consistency between each experiment, the GAC in the adsorption experiments was separated using a vibratory sieve shaker (AS200, RETSCH[®], Haan, Germany). The sieves used had four different mesh sizes, 0.5, 0.71, 1.0, and 1.4 mm, respectively. The parameters used for the vibratory sieve shaker were 10 min for the sieving process with a 10 s interval, and the amplitude for sieving was 1.2 mm. The GAC used for sieving was around 250 g. All fractions were weighed after the separation process to calculate the ratio between each part to the total amount (this step was repeated three times). Of the five fractions thereby obtained, one or two fractions, which accounted for more than 50% of the total GAC, were selected as the working adsorbent (0.71–1.4 mm). Before applying the GAC in adsorption experiment, the GAC was dried at $105 \pm 1\ ^\circ\text{C}$ to a constant weight and later stored in a desiccator.

2.3. Adsorption of Fractionated DOM and Pollutants onto GAC

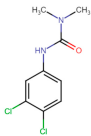
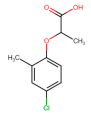
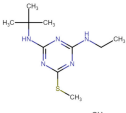
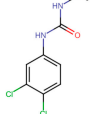
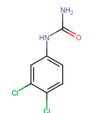
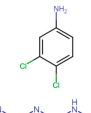
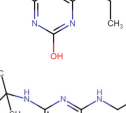
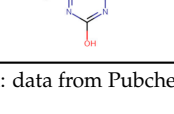
In order to study the adsorption of pollutants in building runoff onto GAC, we selected three fractionated DOM ($>100\ \text{kDa}$, 10–30 kDa, and 3–10 kDa), two heavy metals (Cu^{2+} and Zn^{2+}) relevant to metal roof runoff, as well as three different biocides and their respective biocide transformation products (BTPs). See Table 1. All experiments were performed in triplicate.

The investigation of the adsorption of fractionated DOM onto GAC was performed in glass bottles under shaking conditions of 120 rpm, 24 h (Orbital shaker, SM25, Bühler[®], Bodelshausen, Germany). The solid-to-liquid ratio (GAC/Milli-Q water) of this reaction system was maintained at 2 mg/mL. The concentrations of DOM in the adsorption batch tests were 2, 4, 6, 8, 10, 20, 30, 40, 50, 100, 200, 400, and 600 mgC/L (DOM fraction 3–10 kDa did not include the maximum concentration). For samples with a DOM concentration of less than 40 mgC/L, the test volume was 100 mL (200 mg GAC added); for samples with a DOM concentration of 50 and 100 mgC/L, it was 50 mL (100 mg GAC added); the remaining tests were performed using a volume of 15 mL (30 mg GAC added). The decline in test volume was determined by the limited amount of fractionated DOM stock solution. All of the samples in these experiments contained 10 mM NaCl (Merck[®], Darmstadt, Germany) in order to simulate environmental ionic strength. The pH value of samples with a volume larger than 50 mL was adjusted to 7.0 ± 0.2 . Since the sieved GAC comprised some fine particles which could not be removed using a $0.45\ \mu\text{m}$ filter, measurement of the remaining DOM after adsorption was achieved by calibrating the sample ($0.45\ \mu\text{m}$ filtered) absorbance through calibration curves, which were acquired at 254 nm.

The experiments concerning the adsorption of Cu^{2+} and Zn^{2+} onto GAC were similar to the DOM adsorption experiments. The study was carried out in glass bottles, and the heavy metals added were CuCl_2 (Merck[®], Darmstadt, Germany) and ZnCl_2 (Merck[®], Darmstadt, Germany). The stock solutions were at a concentration of 5 g/L. In the experiments, $200 \pm 0.2\ \text{mg}$ GAC was added into 100 mL Milli-Q water containing 10 mM NaCl. The concentration of Cu^{2+} and Zn^{2+} in the samples was 5, 10, 15, 20, 30, and 40 mg/L,

respectively. The pH value of the samples was adjusted to 6.0 ± 0.2 to minimize the precipitation of Cu^{2+} . All of the samples were shaken at 120 rpm for 24 h to achieve adequate adsorption. The concentration of the remaining heavy metals in each sample was determined via atomic absorption spectroscopy analysis after filtration through a $0.45 \mu\text{m}$ syringe filter and acidification with HNO_3 (Merck[®], Darmstadt, Germany) [29].

Table 1. The biocides/BTPs used and their physicochemical properties.

Chemicals	Molecular Structure ^b	Molecular Formula ^a	Molecular Weight ^a	Water Solubility (mg/L) ^a	LogD (pH = 7) ^b
Diuron		$\text{C}_9\text{H}_{10}\text{Cl}_2\text{N}_2\text{O}$	233.09	37.4–42 (−3.11) ^c	2.53
Mecoprop-p		$\text{C}_{10}\text{H}_{11}\text{ClO}_3$	214.64	880 (0.0) ^c	−0.25
Terbutryn		$\text{C}_{10}\text{H}_{19}\text{N}_5\text{S}$	241.36	35.9 (−3.65) ^c	2.7
1-(3,4-Dichlorophenyl)-3-methylurea (DCPMU)		$\text{C}_8\text{H}_8\text{Cl}_2\text{N}_2\text{O}$	219.06	(−3.08) ^c	2.31
1-(3,4-Dichlorophenyl)urea (DCPU)		$\text{C}_7\text{H}_6\text{Cl}_2\text{N}_2\text{O}$	205.04	(−3.08) ^c	2.09
3,4-Dichloroaniline (DCA)		$\text{C}_6\text{H}_5\text{Cl}_2\text{N}$	162.01	(−2.75) ^c	2.35
Atrazine-desisopropyl-2-hydroxy (DHT)		$\text{C}_5\text{H}_9\text{N}_5\text{O}$	155.16	(−1.8) ^c	0.59
Terbutylazine-2-hydroxy (HAT)		$\text{C}_9\text{H}_{17}\text{N}_5\text{O}$	211.26	(−2.67) ^c	1.94

Notes: a: data from Pubchem; b: calculated data from ChemAxon; c: calculated solubility LogS from ChemAxon.

The organic chemicals used to study the adsorption of biocides and their BTPs onto GAC were purchased from Dr. Ehrenstorfer[®] (Augsburg, Germany). In the experiment, $10 \pm 0.2 \text{ mg}$ of GAC was weighed and added into a 100 mL solution of 10 mM NaCl. The concentrations of biocides and BTPs in the experiments were 5, 10, 15, 20, 30, and 40 mg/L. The stock solution of biocides and BTPs was prepared in methanol (Merck[®], Darmstadt, Germany) at a concentration of 10 g/L, except for atrazine-desisopropyl-2-hydroxy and terbutylazine-2-hydroxy. These two chemicals had lower solubility in methanol; therefore, their stock solutions were prepared at a lower concentration of 2 g/L and was dissolved in a mix of water/MeOH (1:1) containing 0.4% formic acid (Merck[®], Darmstadt, Germany). The pH value of the samples was adjusted to 7.0 ± 0.2 before shaking at 120 rpm for 24 h. Regarding those samples containing Terbutylazine-2-hydroxy, it was observed that the chemical formed a floccule after pH adjustment. To overcome this issue, we added 20 μL of formic acid (Merck[®], Darmstadt, Germany) into these samples ($V_T = 100 \text{ mL}$) after the shaking process and before sampling in order to return it to a dissolved form. The collected samples were analysed via liquid chromatography coupled with mass spectrometry (LC-MS) after a filtration step using $0.22 \mu\text{m}$ syringe filters.

2.4. Pollutants Co-Presence during the Adsorption Process

The evaluation mainly focused on the influence of DOM on the adsorption of heavy metals and biocides onto GAC. We also studied the influence of heavy metals on the adsorption of biocides onto GAC. The concentrations of DOM fractions in the experiments were maintained at 5 mgC/L, which approached the actual concentration in building runoff [30]. The concentration of heavy metals and biocides was 40 mg/L. The experimental settings were the same as those in Section 2.3 with the highest pollutant concentration, i.e., 40 mg/L of heavy metals and biocides. With regard to studying the influence of heavy metals on biocide adsorption onto GAC, the experiment setting was similar. The heavy metals concentration was set to 2 mg/L, which mimics the concentration found in metal roof runoff [3]. The biocide concentrations were prepared at 40 mg/L. Bearing in mind the similarity between BTPs and their parent compounds, only the parent biocides were studied in this section. All experiments were performed in triplicate.

2.5. Liquid Chromatography–Mass Spectrometry Analysis

Targeted LC-MS analysis features high levels of resolution and accuracy for detecting trace organic pollutants in environmental and experimental samples, and it has been widely used to analyse biocides [31–33]. In the present study, it was applied in order to quantify the concentrations of biocides and their transformation products (BTPs) in our samples. The UPLC system used was a PLATINblue from Knauer® (Berlin, Germany). The chromatographic column was a 150 × 3 mm, Kinetex® 2.6 µm PFP 100 Å from Phenomenex® (Aschaffenburg, Germany).

The mass spectrometer used was a triple Quad 6500 from Sciex® operated with Analyst (version, 1.6.2, Sciex®, Framingham, MA, USA). The instrument was operated using a Turbo V® ion source with a TurboIonSpray® ESI probe (Framingham, MA, USA). For the detection of the analytes, we used a targeted MRM method with optimized values for DP, CE, and CXP. Each analyte was identified using a quantifier and qualifier transition, in addition to a heavy isotope internal standard. The mobile phase was composed of a gradient of Milli-Q water and LC-MS grade methanol (Merck®, Darmstadt, Germany). Both solvents were supplemented with formic acid to reach a final concentration of 0.1%. The flow rate used was 0.7 mL/min.

2.6. Adsorption Modelling using Freundlich and Langmuir Equations

The Langmuir and Freundlich equations are the two most frequently used models in adsorption studies [34], in the literature; they have been used to describe the adsorption of pollutants onto GAC [35,36], powder activated carbon [37], and biochar [38].

The expression of the Langmuir model (1) is as follows:

$$q_e = (q_0 \times K_L \times C_e) / (1 + K_L \times C_e), \quad (1)$$

where “ q_e ” is the adsorbed amount of pollutant at equilibrium in mg/g, “ q_0 ” is the maximum adsorption of pollutants to a given adsorbent in mg/g, and “ K_L ” is the Langmuir constant in L/mg, which means the affinity of adsorbate to the adsorbent [39]. “ C_e ” is the equilibrium concentration of adsorbate.

The expression of the Freundlich model (2) is as follows:

$$q_e = b \times C_e^{1/n}, \quad (2)$$

where “ q_e ” and “ C_e ” are the same variables as in the Langmuir model, “ b ” and “ n ” are constants for a given adsorbate and adsorbent at a given experimental condition, in which “ b ” means the adsorption affinity and “ n ” means the heterogeneity of the adsorbent surface [40].

3. Results and Discussion

3.1. DOM and Granular Activated Carbon Prepared

After the centrifugation process, five different DOM fractions were obtained (>100 kDa, 30–100 kDa, 10–30 kDa, 3–10 kDa, and <3 kDa). The DOM fractionation results showed that the majority of the obtained DOM belonged to the fractions >100 kDa (60.8%), 10–30 kDa (15.4%) and 3–10 kDa (20.6%), where they accounted for 96.8% of total DOM, while the fractions in the range of 30–100 kDa (1.4%) and <3 kDa (1.8%) exhibited significantly lower values. Hence, we decided to only use the more significant part of the DOM fractions, in this case >100 kDa, 10–30 kDa, and 3–10 kDa.

The separation of GAC according to particle size was successfully achieved by sieving. We thus obtained five different fractions, which were classified as: >1.4 mm, 1.0–1.4 mm, 0.71–1.0 mm, 0.5–0.71 mm, and <0.5 mm. The respective fractions accounted for $23.3 \pm 2.8\%$, $39.4 \pm 0.6\%$, $26.0 \pm 1.7\%$, $9.3 \pm 1.3\%$, and $1.9 \pm 0.5\%$ of the total GAC. It was noteworthy that no single fraction accounted for more than 50% by itself. This last finding made it necessary to mix at least two fractions together in order to prepare a representative GAC for the experiments. We therefore selected the fractions 1.0–1.4 mm and 0.71–1.0 mm, which together accounted for around 65.4% of the total GAC. Given its large size, the fraction >1.4 mm was not appropriate for our experiments, thus leading to weighing difficulties along with uniformity issues when compared with the whole set of GAC. We also found difficulties in working with fractions in the range of <0.71 mm, which was scarce and not representative of the experiment. Therefore, both fractions were discarded.

3.2. The Adsorption of DOM onto GAC

Figure 1a shows the results of the adsorption of DOM fractions >100 kDa, 10–30 kDa, and 3–10 kDa onto GAC. Unsurprisingly, DOM adsorption exhibited a correlation with concentration. The 3–10 kDa fraction appears to have reached a saturation at 400–500 mgC/L, whereas the other fractions continued to adsorb DOM at the concentrations studied. Applying DOM at a concentration <400 mgC/L clearly showed a descending adsorption tendency of the DOM fractions onto the GAC, in which the 3–10 kDa fraction was the most efficient, followed by 10–30 kDa, and >100 kDa. Such a tendency was also reflected by the half adsorption of DOM, where 50% adsorption for DOM fraction 3–10 kDa, 10–30 kDa, and >100 kDa was found at around 20 mgC/L, 8 mgC/L, and 5 mgC/L, respectively.

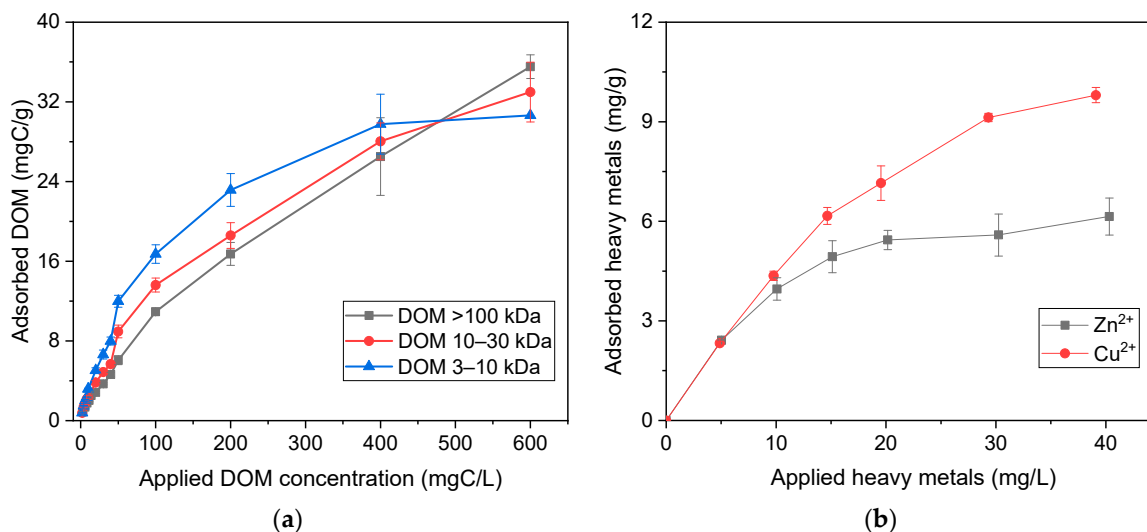


Figure 1. Adsorption curve for DOM and heavy metals. (a) The adsorption of different DOM fractions to 200 mg GAC at various concentrations in 100 mL Milli-Q water (The data point at 600 mgC/L for the 3–10 kDa fraction is an estimated result according to the Langmuir modelling equation, because the stock solution concentration of this fraction was only 567 mgC/L). (b) The adsorption of Cu²⁺ and Zn²⁺ to 200 mg GAC at various concentration in 100 mL Milli-Q water.

The preferential adsorption of small-size DOM fraction onto GAC has also been reported by Schreiber et al., 2005 [41] and Shimabuku et al., 2017 [42]. The reason is that GAC is a porous material, which facilitates the interaction with the smaller DOM fraction (3–10 kDa) due to its size. As a result, it is quite likely that the smaller DOM fraction is able to access binding sites in the GAC pores not available to the large molecules. By increasing the concentration from 2 to 600 mgC/L, the adsorption difference between different fractions onto the GAC grows until 200 mgC/L; above 200 mgC/L, the variance initially shrinks before reversing at around 500 mgC/L, finally exhibiting the highest adsorption tendency from the >100 kDa fraction, with the lowest being the 3–10 kDa fraction. The change during the adsorption process is very likely due to the gradual saturation of GAC. The added DOM concentration was initially low, which meant that the binding sites at the surface of the GAC were sufficient to adsorb the DOM fractions. It is therefore proposed that, at low concentrations, a substantial amount of DOM is attached on the surface of GAC, while a minor portion of DOM is accessing the pores of the GAC. Considering the low DOM concentration added (2 mgC/L), the difference between DOM fractions adsorption was very small. For example, at 2 mgC/L, the 3–10 kDa fraction adsorbed 79%, while the 10–30 kDa fraction adsorbed 78%. The >100 kDa fraction adsorbed an amount of around 70%. By increasing the DOM concentration, the surface binding sites are gradually occupied. Due to the clogging effect, which prevents the entrance of other large DOM molecules into the GAC pores, however, smaller DOM fractions are still able to access the binding sites inside the pores. The result was an adsorption difference between DOM fractions, which reached a maximum at 200 mgC/L in the experiment. At this concentration, the GAC adsorbed 3.35 mg/g more DOM of 3–10 kDa than of >100 kDa. When the DOM concentration continued to increase, the MW of DOM began to play an important role, i.e., that a large molecular weight for DOM will produce more carbon absorption due to its polymeric carbon contain. As before, at concentrations larger than 200 mgC/L, an increasing DOM concentration enhances the adsorption of all DOM fractions onto the GAC. However, the feature of large DOM fraction containing more carbon atoms in one molecule outweighs the adsorption enhancement by accessing the pores. Consequently, at 600 mgC/L, the highest adsorption was observed for the DOM fraction > 100 kDa of 35.5 mg/g, followed by 33.0 mg/g for 10–30 kDa. In the case of the 3–10 kDa fraction, we estimated the value of 30.5 mg/g using the Langmuir equation (Figure 1a) because the stock solution concentration of this fraction was only 567 mgC/L.

The Langmuir modelling results determined the estimated maximum adsorption of each DOM fraction onto the GAC, whereby we found that the >100 kDa fraction can adsorb 59.4 ± 5.2 mg/g. The DOM 10–30 kDa fraction can adsorb 41.3 ± 2.4 mg/g, and the amount able to be adsorbed in the 3–10 kDa fraction was 34.3 ± 1.7 mg/g. These results are in accordance with previous research studying the adsorption of algal organic matter onto GAC, which obtained an adsorption of 31.45 mg/g [43]. The affinity of the adsorbate to the adsorbent (“ K_L ” value) increases with a decreasing DOM MW, which means that the smaller DOM fraction has a higher affinity for the GAC. The minimum R^2 value in the Langmuir modelling is 0.985, which suggests that the adsorption processes are well-fitted using the Langmuir equation. The “ n ” constant based on Freundlich modelling for the adsorption of DOM > 100 kDa fraction onto the GAC was 1.50 ± 0.03 . The results from the DOM 10–30 kDa and 3–10 kDa fractions were 1.89 ± 0.08 and 2.15 ± 0.14 , respectively. Since the “ n ” value represents the heterogeneity in the adsorption process, a larger value means that the system is more heterogeneous [40]. The difference between “ n ” values implies that the smallest DOM fraction had different binding sites than the large ones. This conclusion is supported by the result in Figure 1a, which shows that, at the same concentration below 200 mgC/L, the pore structure in the GAC provided additional binding sites for the smaller DOM fractions. The ascending “ b ” values along with the descending DOM MW leads to the same conclusion of the Langmuir modelling, i.e., that the smaller fraction interacts more with the GAC than the large fractions. The R^2 values of the Freundlich modelling are above 0.975, which meant a good adsorption fitting result for each fraction.

3.3. The Adsorption of Heavy Metals onto GAC

The adsorption of heavy metals onto the GAC behaves similarly to the adsorption of DOM onto the GAC (Figure 1b). Strong adsorption was observed at the beginning, with a low concentration of heavy metals. For both Cu²⁺ and Zn²⁺, at 5 mg/L, only 5% of the heavy metals was still found in the dissolved form. With the increase in the heavy metal concentration, the adsorption increased gradually for both Cu²⁺ and Zn²⁺. In the experiment at concentrations higher than 5 mg/L, Cu²⁺ exhibited a higher affinity to the GAC than Zn²⁺. At 40 mg/L heavy metal concentration, we observed the largest affinity difference in the adsorption of 60 μmol/g; at this concentration, 50% of applied Cu²⁺ was adsorbed and the amount adsorbed for Zn²⁺ was 30%. The Langmuir and Freundlich modelling results are shown in Table 2. According to the Langmuir modelling, the estimated maximum adsorption of Cu²⁺ and Zn²⁺ onto the GAC is around 157 and 85.7 μmol/g, respectively. This result is in accordance with the results found by Sountharajah et al., 2015 [44], who reported a Langmuir maximum adsorption of Cu²⁺ and Zn²⁺ onto the GAC at 186 and 50.5 μmol/g, respectively. It has been noted that the adsorption of Cu²⁺ onto the GAC is always stronger than that of Zn²⁺. The higher adsorption affinity of Cu²⁺ has also been reported by studies investigating Cu²⁺ and Zn²⁺ adsorption onto biochars [45–47]. Interestingly, the adsorption affinity difference between Cu²⁺ and Zn²⁺ is well described by the “b” value in the Freundlich model (a higher value represents a stronger adsorption), but the “K_L” values in the Langmuir model failed to explain the absorption difference between the Cu²⁺ and Zn²⁺. This is because several kinds of polar functional groups in the GAC are involved in the adsorption of Cu²⁺ and Zn²⁺, e.g., phenolic and carboxylic groups [48]. Different functional groups provide different binding sites, i.e., a heterogeneous GAC surface to catch heavy metal cations. As previously mentioned, the Freundlich model is proposed for heterogeneous adsorption, and the Langmuir model is more appropriate for homogeneous adsorption. Therefore, the Freundlich model fits the Cu²⁺/Zn²⁺ adsorption data well (R² = 0.984/0.961), as expected. Theoretically, the Langmuir model should provide a less satisfactory result for both Cu²⁺ and Zn²⁺. However, the fitting for Cu²⁺ adsorption onto GAC was still quite good and was due to the strong binding affinity of Cu²⁺ toward GAC (the heterogeneity at the GAC surface becomes relatively not significant for Cu²⁺). At the same time, this was not the case for the Zn²⁺ for reason of its weaker binding capability (the GAC surface is heterogeneous for Zn²⁺). Consequently, the Langmuir model poorly describes the adsorption affinity difference between Cu²⁺ and Zn²⁺ onto the GAC by way of the “K_L” value. The relative difference at the surface of the GAC for Cu²⁺ and Zn²⁺ is proved by the “n” values from the Freundlich model, in which case the Zn²⁺ had a higher value, i.e., a more heterogeneous surface.

Table 2. Pollutants GAC adsorption modelling results by the Langmuir and Freundlich equations.

Compounds	Langmuir Modelling			Freundlich Modelling		
	q ₀ (mg/g, μmol/g)	K _L	R ²	b	n	R ²
DOM > 100 K	59.4 ± 5.2 ^a	(2.58 ± 0.42) × 10 ⁻³	0.991	0.55 ± 0.04	1.50 ± 0.03	0.998
DOM 10–30 K	41.4 ± 2.4 ^a	(6.33 ± 0.92) × 10 ⁻³	0.986	1.23 ± 0.15	1.89 ± 0.08	0.990
DOM 3–10 K	34.3 ± 1.7 ^a	(15.6 ± 2.02) × 10 ⁻³	0.985	2.09 ± 0.31	2.15 ± 0.14	0.975
Cu ²⁺	157.4 ± 0.5 ^b	0.72 ± 0.16	0.974	4.42 ± 0.25	3.52 ± 0.31	0.984
Zn ²⁺	85.7 ± 4.6 ^b	2.56 ± 1.15	0.823	3.49 ± 0.17	5.72 ± 0.61	0.961
Diuron	1621.7 ± 437.6 ^b	0.026 ± 0.01	0.978	1.41 ± 0.25	1.35 ± 0.11	0.983
Mecoprop	N.A.	N.A.	N.A.	0.222 ± 0.06	0.992 ± 0.09	0.981
Terbutryn	219.2 ± 46.0 ^b	0.29 ± 0.27	0.707	23.7 ± 11.0	4.96 ± 4.01	0.623
DCPMU	2506.2 ± 310.4 ^b	0.021 ± 0.004	0.997	14.8 ± 1.2	1.25 ± 0.05	0.997
DHT	495.6 ± 362.9 ^b	0.04 ± 0.05	0.763	5.0 ± 3.6	1.56 ± 0.61	0.785
DCPU	304.3 ± 17.9 ^b	0.64 ± 0.20	0.970	34.2 ± 6.0	5.65 ± 2.26	0.919
DCA	2888.8 ± 191.3 ^b	0.059 ± 0.01	0.997	35.4 ± 1.5	1.48 ± 0.04	0.998
HAT	N.A.	N.A.	N.A.	9.76 ± 1.7	1.52 ± 0.13	0.982

Notes: N.A. means not available; a: the unit is mg/g; b: the unit is μmol/g.

3.4. The Adsorption of Biocides and Biocide Transformation Products onto GAC

Figure 2 illustrates the results of biocides and biocides transformation products (BTPs) being adsorbed onto GAC. In our study, we applied three biocides with different chemical natures. We therefore used two main groups, benzene and triazine derivatives (Figure 2C). Hence, we tested terbutryn, diuron, and mecoprop-p. In the case of BTPs, we used diuron (DCPMU, DCPU DCA) and terbutryn (DHT, HAT) derivatives.

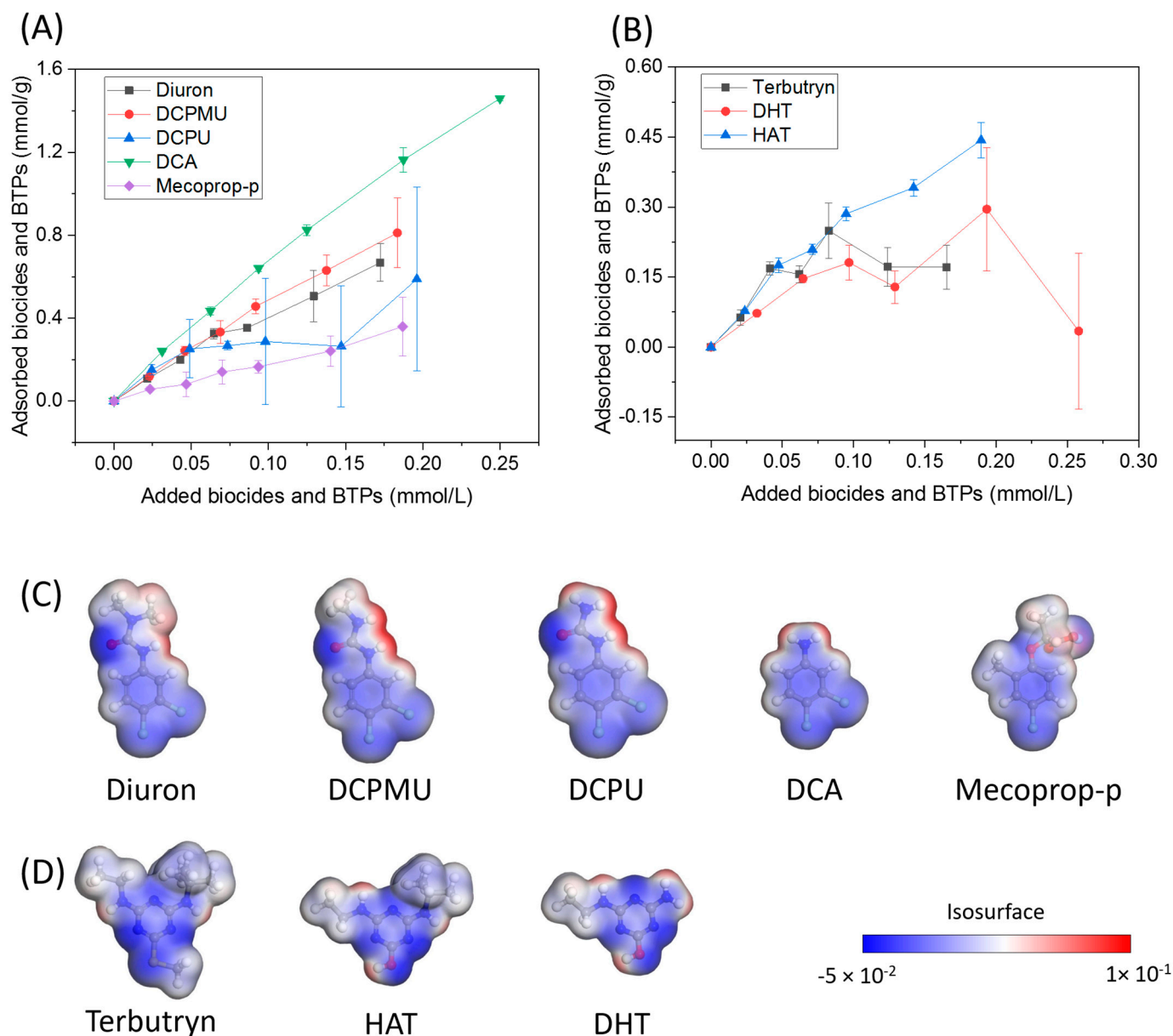


Figure 2. The adsorption of biocides/BTPs onto GAC and biocides/BTPs charge distribution. (A) The adsorption of benzene related biocides and BTPs onto 10 mg GAC in 100 mL Milli-Q water; (B) The adsorption of triazine related biocides and BTPs onto 10 mg GAC in 100 mL Milli-Q water. (C,D) Charge distribution of biocides and their BTPs used in this study, calculated via Materials Studio with module DMol3; blue indicates a charge abundant area.

In contrast to the adsorption of DOM or heavy metals onto GAC, the adsorption of biocides and BTPs toward GAC commonly exhibits no clear saturation trend, except for terbutryn, which had a saturation point at 0.125 mmol/L (Figure 2B). At higher concentrations, DHT presented a behaviour which was not informative in determining whether GAC reached a saturation point (Figure 2B). For the other biocides and transformation products,

we observed a collinearity between concentration and adsorption (Figure 2A,B). In the experiment, the highest adsorption onto GAC was found for the chemical DCA, followed by (in decreasing order) DCPMU, diuron, DCPU, HAT, mecoprop-p, DHT, and terbutryn. It is noteworthy that the parent biocide and its transformation products presented similar adsorption capacities. In addition, the benzene-derived biocides (Figure 2C: diuron related chemicals) exhibited a higher adsorption ability than triazine-derived biocides (Figure 2D: terbutryn-related chemicals). The discovery of an adsorption difference between biocide groups (benzene and triazine derivatives) is similar to the result obtained by Baup et al., 2002 [49], who reported a higher adsorption for diuron onto the GAC than atrazine (the atrazine has the same core structure as terbutryn).

The analysis also found that the difference between chemicals adsorption onto GAC cannot be explained by their different LogD values, which is in accordance with findings by Tang et al., 2020 [25]. Usually, a higher LogD value implies a higher hydrophobicity of a molecule and a stronger hydrophobic interaction with GAC; however, the results in this experiment did not fit the LogD prediction because the expected behaviour was not observed when compared with the adsorption. For example, the LogD values for terbutryn, diuron, and mecoprop-p are 2.7, 2.53, and -0.25 , respectively, and the adsorption sequence for them from high to low is diuron > mecoprop-p \geq terbutryn. This inconsistency is also found between diuron/terbutryn and their own transformation products (TP) (see Table 1 and Figure 2). This phenomenon is mainly due to the involvement of spatial hindrance from biocides and the BTPs. For all three biocides and their TPs, they have benzene or triazine ring structures, thus enabling the interaction with GAC through π - π interactions [50]. However, their contact with the surface of GAC is influenced by their own three-dimensional molecular structure. For example, as shown in Figure 2C,D, terbutryn, mecoprop-p, and HAT have a bulky structure, which very likely plays a detrimental role in the interaction between the molecules and the GAC surface. In contrast, diuron and DCPMU have a planar three-dimensional distribution due to the absence of bulky groups (iso-propyl at terbutryn), which enhances the interaction between the adsorbent surface (GAC) and diuron and DCPMU. Consequently, diuron-like compounds can attach to the GAC surface more easily and exhibit a higher adsorption capacity—despite benzene and triazine derived biocides supposedly having a similar π - π interaction ability based on the similar charge distribution around the ring structures. The DCA exhibited the highest adsorption among these compounds, which further confirms the above assumption that planar three-dimensional distribution can directly affect the interaction between biocides/BTPs and the GAC. The influence of the three-dimensional molecular structure was also proposed by Apul et al., 2013 [51] after they normalized the properties of phenanthrene and biphenyl and found that the hydrophobic interaction was not the only factor controlling the adsorption process. Mecoprop-p, which has a negative LogD value (-0.25), nevertheless presented a higher adsorption ability than terbutryn; this outcome can be attributed to the carboxylic acid-related hydrogen bonding [52] and the possible anion- π interaction [53] with GAC.

The Langmuir and Freundlich fitting results of biocides and BTPs adsorption onto GAC are listed in Table 2. Not all of the data were as satisfactory as those obtained from the DOM fractions and heavy metals adsorption experiments, but the data still described most of the adsorption processes in a quantitative way. The estimated diuron adsorption capacity was around $1622 \mu\text{mol/g}$, which is higher than the result reported by Al Bahri et al., 2016 [54], but closer to the data from de Souza and dos Santos, 2020 [55] using commercial organophilic clay as an adsorbent. The estimated adsorption capacity for DCA, the chemical with the highest adsorption, was around $2900 \mu\text{mol/g}$, which was significantly higher than the data from terbutryn ($219 \mu\text{mol/g}$). By comparing the Langmuir and Freundlich modelling results, we observed that the Freundlich model fits better than the Langmuir model due to the heterogeneity in the adsorption process (GAC surface), which is similar to the result obtained by McGinley et al., 2022 [56], who claimed that the Freundlich model was the best one for describing the adsorption of herbicides onto GAC.

3.5. The Influence of Co-Presence on the Adsorption Processes

In evaluating the influence of other substances (DOM and heavy metals) also present in the building runoff on the adsorption of target substance onto GAC, the concentration of the influencing factor was designed to mimic that found in the runoff, as shown in Figure 3.

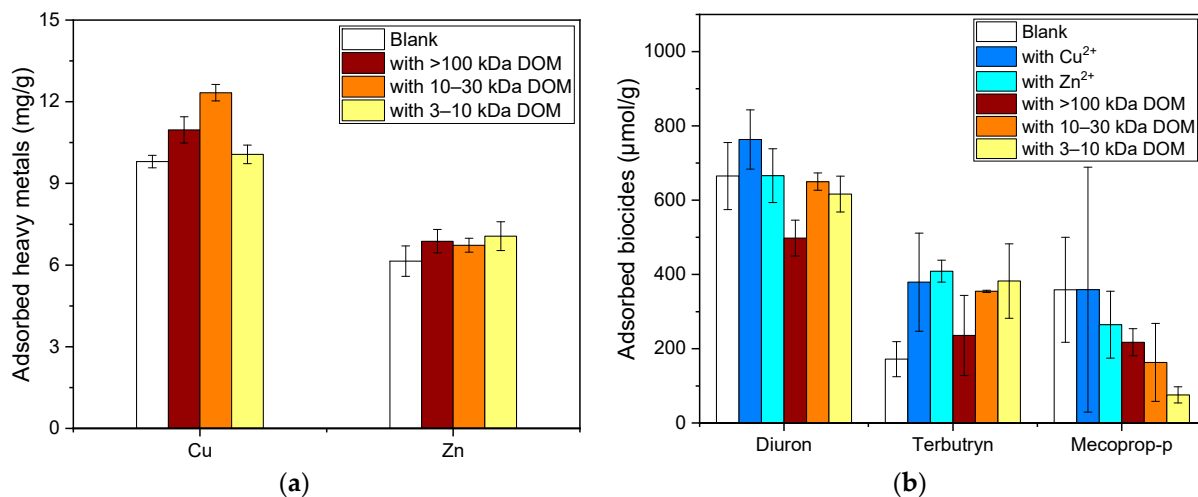


Figure 3. Influence of co-presence on the adsorption processes. (a) The influence of the presence of various DOM fractions (5 mg/L) on the adsorption of heavy metals (40 mg/L) onto 200 mg GAC in 100 mL Milli-Q water. (b) The influence of the presence of heavy metals (2 mg/L) and various DOM fractions (5 mg/L) on the adsorption of diuron, terbutryn, and mecoprop-p (40 mg/L) onto 10 mg GAC in 100 mL Milli-Q water. The large deviation for mecoprop-p could also be a result of methodological error.

According to the adsorption curves in Figure 1a, the application of 5 mgC/L of various DOM fractions were easily absorbed by 200 mg GAC, which means that more than 50% of the DOM fractions were adsorbed. It is also noteworthy that, as shown in Figure 3a, the presence of DOM was able to enhance the adsorption of heavy metals. For Cu²⁺, the greatest enhancement was found in the 10–30 kDa fraction (25.8%) followed by >100 kDa fraction (11.9%) and 3–10 kDa fraction (2.7%). This outcome is likely due to the oxygen-containing functional groups in the adsorbed DOM providing additional binding sites for Cu²⁺ [57], thus increasing its adsorption onto the GAC. The slightly smaller adsorption of the >100 kDa fraction than the 10–30 kDa fraction can be explained by the severer blockage effect of larger DOM molecules at the entrance of GAC pores, which results in a higher loss of binding sites inside the GAC pore structures for Cu²⁺, thus leading to the observation of a reduced Cu²⁺ adsorption. The 3–10 kDa fraction showed no clear enhancement in the Cu²⁺ adsorption because it presents a more severe blockage effect than the other two fractions. The 3–10 kDa fraction has the smallest molecular size. When applying DOM fractions at the same concentration (milligram carbon per liter), it provides the largest number of molecules, i.e., the most severe blockage effect. Furthermore, the increased binding sites from 3–10 kDa fraction cannot offset the above side effect. Eventually, the presence of the smallest DOM fraction exhibits little promotion of Cu²⁺ adsorption. By way of comparison with previous studies, Genç-Fuhrman et al., 2016 [58] and Esfandiari et al., 2022 [59] reported a negative impact of DOM on the adsorption of Cu²⁺ to adsorbents, which is the opposite of the results obtained in this study. The main reason for these conflicting results is the higher concentration of the applied DOM (around 20 mgC/L) or the use of a less active adsorbent such as biochar. As a result, a major part of DOM was in dissolved form; thus, DOM and GAC competed for Cu²⁺, which reduced the Cu²⁺ adsorption. Given that Zn²⁺ showed a minor affinity to adsorption onto the GAC, it was less affected (average adsorption increase of 0.75 mg/g) by the presence of DOM and the blockage effect in the small pores.

Figure 3b illustrates the influence of heavy metals on the adsorption of biocides onto the GAC. The adsorption of diuron onto GAC was enhanced by 14.8% in the presence of Cu^{2+} but almost unaffected by the Zn^{2+} . Regarding terbutryn, the presence of heavy metals doubled its adsorption onto the GAC (increasing 120% for Cu^{2+} and 138% for Zn^{2+}). As for mecoprop-p, the presence of Cu^{2+} did not considerably affect its average adsorption (with a big deviation in the data set). However, in the presence of Zn^{2+} , mecoprop-p decreased the adsorption by 26.2%. As previously mentioned, the heavy metals interact with the GAC through the oxygen-containing functional groups. In fact, these functional groups are related to hydrogen bonding, which can be formed inter- and intramolecularly. The binding of heavy metals with GAC means the destruction of intramolecular hydrogen bonding inside the GAC, as well the hydrogen bonding between the GAC and the biocides. The result of the H bonding destruction is the exposure of electric charge abundant interaction sites. This change explains the alteration of biocide adsorption onto the GAC in the presence of heavy metals. For example, diuron and its slightly improved adsorption in the presence of Cu^{2+} is the result of increased π - π interaction sites due to the destruction of intramolecular hydrogen bonding. The minor affinity of Zn^{2+} toward the GAC led to insignificant changes in the adsorption of diuron onto GAC, with values almost identical to those found in the control condition (blank). Correspondingly, the significant enhancement of terbutryn adsorption can also be explained by the increased interaction sites originating from the intramolecular hydrogen bonding due to the binding of heavy metals. The reason for an adverse effect of the Zn^{2+} presence on the mecoprop-p adsorption is that some binding sites at the GAC surface were no longer able to act as hydrogen bonding donor because they were occupied by Zn^{2+} . The role that Cu^{2+} plays in the mecoprop-p adsorption is complex, as it competes with the mecoprop-p for the functional groups. At the same time, it can be assumed that Cu^{2+} is able to build a cation bridge to connect the mecoprop-p and the GAC. An insignificant effect on the adsorption of mecoprop-p caused by the presence of Cu^{2+} is therefore also reasonable. It should be noted that the different reaction of biocides adsorbing onto the GAC in the presence of heavy metals is due to the combined effect of π - π interaction and hydrogen bonding. A few similar positive and negative effects have been reported in previous studies. For instance, Zheng et al., 2018 [60] found that Cu^{2+} increased the adsorption of methyl orange onto a modified GAC material. The presence of heavy metals reduced the adsorption of polycyclic aromatic hydrocarbons onto the GAC [61]. Cr(III) and atrazine together exhibited a competitive adsorption onto the activated carbons [62], and others.

Similar to the influence of heavy metals on the adsorption of biocides onto the GAC, DOM fractions have a differing effect on the biocide adsorption processes (Figure 3b). The adsorption of diuron was inhibited by 25.1% in the presence of the DOM > 100 kDa fraction. The 10–30 kDa fraction did not exhibit much inhibition, and an inhibition of 7.3% was observed in the 3–10 kDa fraction. For terbutryn, the adsorption onto GAC was enhanced by all three DOM fractions. It was observed that the smaller MW of DOM has the best enhancement for the terbutryn adsorption onto GAC. The enhanced adsorptions were 37% (>100 kDa), 106% (10–30 kDa), and 122% (3–10 kDa), respectively. In contrast with terbutryn adsorption, the adsorption of mecoprop-p was clearly inhibited by the DOM fractions. The smaller of DOM MW the more inhibition was found. These three DOM fractions inhibited the mecoprop-p adsorption by 39.4% (>100 kDa), 54.5% (10–30 kDa), and 78.9% (3–10 kDa), respectively. Of all three biocides, the less affected adsorption of diuron in the presence of DOM is because of its strong π - π interaction with the GAC, which resists the competition from DOM (except for >100 kDa DOM, since the polymeric form covers up some active sites). The enhanced terbutryn adsorption was due to the intramolecular hydrogen bonding inside the GAC being destroyed by forming new intermolecular hydrogen bonding between the GAC and the DOM. As a result, the GAC provides additional π - π interaction binding sites for terbutryn. The inhibition of mecoprop-p adsorption resulted from the direct competition of hydrogen bonding sites at the GAC surface with DOM. The varying influence of DOM on the adsorption of biocides onto the GAC was similar

to that observed in previous studies. For example, Radian and Mishael, 2012 [63] found that the GAC adsorption kinetic of pyrene at equilibrium did not exhibit much difference when the DOM was added. However, a study by Lin et al., 2017 [64] reported that the presence of DOM hindered the removal of ibuprofen and sulfamethoxazole by way of the biochar. At the same time, the result by Jin et al., 2018 [65] implied that the presence of humic acid increased the adsorption of tetracycline and ciprofloxacin onto the activated carbon. Overall, the DOM affects the biocides adsorption by competing and providing the hydrogen bonding/ π - π interaction sites at the same time, thus resulting in different or even adverse biocide adsorption responses.

4. Conclusions

The adsorption of DOM onto GAC is related to both their MW and the DOM concentration applied in the adsorption experiment. At low DOM concentrations, the smaller fraction of DOM adsorbs more because it is able to access to the small pores inside the GAC. At high DOM concentrations, the larger fraction adsorbs more because the larger DOM molecule carries more carbon atoms. The adsorption behaviour of heavy metals as pollutants onto GAC differs: Cu^{2+} showed a higher affinity for GAC than Zn^{2+} . In this study, the Langmuir and Freundlich equations were good models for describing the adsorption of DOM and heavy metals onto GAC. The Langmuir equation successfully provided the estimated maximum adsorption of pollutants onto GAC. The Freundlich equation effectively described the heterogeneity of the GAC surface to the adsorbates. Regarding the adsorption of biocides and the corresponding TPs as pollutants onto GAC, they had a strong correlation in their adsorption capacity. At the same time, we conclude that the LogD values of biocides/BTPs themselves were not enough to explain the adsorption differences. Another key factor in describing the biocides/BTPs adsorption is their three-dimensional molecular structure. Biocides/BTPs having a more planar 3D structure, which will tend to facilitate the π - π interactions between GAC and the biocides/BTPs.

The influence of the simultaneous occurrence of different substances on the adsorption of target pollutants onto GAC was able to be demonstrated. (1) The presence of DOM enhanced the adsorption of heavy metals onto GAC at low DOM concentrations. (2) The DOM influence on the adsorption of biocides differs depending on the compounds used because both hydrophobic interaction and hydrogen bonding are involved in the adsorption process and these two mechanisms respond differently to the presence of DOM. As a result, no clear trend was observed. (3) The influence of the presence of heavy metals on the adsorption of biocides also depends on the chemical structure of the biocides, which is due to the same reason as described in (2). Based on these findings, it can be stated that, in adsorption experiments used to develop decentralized stormwater treatment facilities, it is important that experiments be performed using individual substances while also taking matrix influences into consideration.

Overall, the GAC is an ideal adsorbent material for the retention of pollutants in building runoff with great potential. When analysing the adsorption of biocides, it is important to consider the influence of biocides molecular 3D structure. The effect of the presence of DOM and heavy metals on the adsorption of biocides should be carefully distinguished according to the biocides used. This study is a fundamental part of building runoff treatment system design. The follow-up work will focus on studying the adsorption of biocides at real runoff concentration, optimizing the conditions for GAC utilization, studying the effect of temperature on adsorption, and analysing the regeneration and desorption of the GAC.

Author Contributions: Conceptualization, P.Z.; methodology, P.Z.; validation, P.Z., I.S. and B.H.; formal analysis, P.Z. and T.Z.; investigation, P.Z. and T.Z.; resources, B.H.; data curation, P.Z. and I.S.; writing—original draft preparation, P.Z.; writing—review and editing, B.H. and I.S.; visualization, P.Z.; supervision, B.H. and I.S.; project administration, B.H.; funding acquisition, P.Z. and B.H. All authors have read and agreed to the published version of the manuscript.

Funding: This research was funded by a scholarship for Panfeng Zhu from China Scholarship Council.

Data Availability Statement: The data presented in this study are available on request from the corresponding author. The data are not publicly available due to privacy.

Acknowledgments: Thanks for the support from Chemviron Carbon Ltd. for providing granular activated carbon Cyclecarb 301.

Conflicts of Interest: The authors declare no conflict of interest.

References

1. Luthy, R.G.; Sharvelle, S.; Dillon, P. Urban Stormwater to Enhance Water Supply. *Environ. Sci. Technol.* **2019**, *53*, 5534–5542. [[CrossRef](#)]
2. Zhang, D.; Gersberg, R.M.; Ng, W.J.; Tan, S.K. Conventional and Decentralized Urban Stormwater Management: A Comparison through Case Studies of Singapore and Berlin, Germany. *Urban Water J.* **2017**, *14*, 113–124. [[CrossRef](#)]
3. Galster, S.; Helmreich, B. Copper and Zinc as Roofing Materials—A Review on the Occurrence and Mitigation Measures of Runoff Pollution. *Water* **2022**, *14*, 291. [[CrossRef](#)]
4. Athanasiadis, K.; Horn, H.; Helmreich, B. A Field Study on the First Flush Effect of Copper Roof Runoff. *Corros. Sci.* **2010**, *52*, 21–29. [[CrossRef](#)]
5. Charters, F.J.; Cochrane, T.A.; O’Sullivan, A.D. The Influence of Urban Surface Type and Characteristics on Runoff Water Quality. *Sci. Total Environ.* **2021**, *755*, 142470. [[CrossRef](#)]
6. Müller, A.; Österlund, H.; Nordqvist, K.; Marsalek, J.; Viklander, M. Building Surface Materials as Sources of Micropollutants in Building Runoff: A Pilot Study. *Sci. Total Environ.* **2019**, *680*, 190–197. [[CrossRef](#)]
7. Styszko, K.; Bollmann, U.E.; Bester, K. Leaching of Biocides from Polymer Renders under Wet/Dry Cycles—Rates and Mechanisms. *Chemosphere* **2015**, *138*, 609–615. [[CrossRef](#)]
8. Pajjens, C.; Bressy, A.; Frère, B.; Moilleron, R. Biocide Emissions from Building Materials during Wet Weather: Identification of Substances, Mechanism of Release and Transfer to the Aquatic Environment. *Environ. Sci. Pollut. Res.* **2020**, *27*, 3768–3791. [[CrossRef](#)]
9. Uhlig, S.; Colson, B.; Schoknecht, U. A Mathematical Approach for the Analysis of Data Obtained from the Monitoring of Biocides Leached from Treated Materials Exposed to Outdoor Conditions. *Chemosphere* **2019**, *228*, 271–277. [[CrossRef](#)]
10. Vega-Garcia, P.; Schwerd, R.; Scherer, C.; Schwitalla, C.; Johann, S.; Rommel, S.H.; Helmreich, B. Influence of Façade Orientation on the Leaching of Biocides from Building Façades Covered with Mortars and Plasters. *Sci. Total Environ.* **2020**, *734*, 139465. [[CrossRef](#)]
11. Linke, F.; Olsson, O.; Preusser, F.; Kümmerer, K.; Schnarr, L.; Bork, M.; Lange, J. Sources and Pathways of Biocides and Their Transformation Products in Urban Storm Water Infrastructure of a 2 Ha Urban District. *Hydrol. Earth Syst. Sci.* **2021**, *25*, 4495–4512. [[CrossRef](#)]
12. Wicke, D.; Tatis-Muvdi, R.; Rouault, P.; Zerbball-van Baar, P.; Dünnbier, U.; Rohr, M.; Burkhardt, M. Emissions from Building Materials—A Threat to the Environment? *Water* **2022**, *14*, 303. [[CrossRef](#)]
13. Burkhardt, M.; Zuleeg, S.; Vonbank, R.; Bester, K.; Carmeliet, J.; Boller, M.; Wangler, T. Leaching of Biocides from Façades under Natural Weather Conditions. *Environ. Sci. Technol.* **2012**, *46*, 5497–5503. [[CrossRef](#)] [[PubMed](#)]
14. Bucheli, T.D.; Müller, S.R.; Voegelin, A.; Schwarzenbach, R.P. Bituminous Roof Sealing Membranes as Major Sources of the Herbicide (R,S)-Mecoprop in Roof Runoff Waters: Potential Contamination of Groundwater and Surface Waters. *Environ. Sci. Technol.* **1998**, *32*, 3465–3471. [[CrossRef](#)]
15. Burkhardt, M.; Kupper, T.; Hean, S.; Haag, R.; Schmid, P.; Haag, R.; Rossi, L.; Boller, M. *Release of Biocides from Urban Areas into Aquatic Systems*; IWA Newsletter: London, UK, 2007; pp. 15–17.
16. Schwerd, R.; Hübner, S.; Schwitalla, C.; Scherer, C. Freisetzung von Mecoprop aus Polymerbitumendachbahnen. In *Aqua Urbanica Congerence Proceedings 2018*; Technical University of Kaiserslautern: Kaiserslautern, Germany, 2018; pp. 317–320.
17. Fernández-Calviño, D.; Rousk, J.; Bååth, E.; Bollmann, U.E.; Bester, K.; Brandt, K.K. Isothiazolinone Inhibition of Soil Microbial Activity Persists despite Biocide Dissipation. *Soil Biol. Biochem.* **2023**, *178*, 108957. [[CrossRef](#)]
18. Vega-Garcia, P.; Lok, C.S.C.; Marhoon, A.; Schwerd, R.; Johann, S.; Helmreich, B. Modelling the Environmental Fate and Behavior of Biocides Used in Façades Covered with Mortars and Plasters and Their Transformation Products. *Build. Environ.* **2022**, *216*, 108991. [[CrossRef](#)]
19. Bork, M.; Lange, J.; Graf-Rosenfellner, M.; Hensen, B.; Olsson, O.; Hartung, T.; Fernández-Pascual, E.; Lang, F. Urban Storm Water Infiltration Systems Are Not Reliable Sinks for Biocides: Evidence from Column Experiments. *Sci. Rep.* **2021**, *11*, 7242. [[CrossRef](#)] [[PubMed](#)]
20. Ekanayake, D.; Loganathan, P.; Johir, M.A.H.; Kandasamy, J.; Vigneswaran, S. Enhanced Removal of Nutrients, Heavy Metals, and PAH from Synthetic Stormwater by Incorporating Different Adsorbents into a Filter Media. *Water Air Soil Pollut.* **2021**, *232*, 96. [[CrossRef](#)]
21. Ulrich, B.A.; Im, E.A.; Werner, D.; Higgins, C.P. Biochar and Activated Carbon for Enhanced Trace Organic Contaminant Retention in Stormwater Infiltration Systems. *Environ. Sci. Technol.* **2015**, *49*, 6222–6230. [[CrossRef](#)]

22. Chen, J.P.; Wu, S. Simultaneous Adsorption of Copper Ions and Humic Acid onto an Activated Carbon. *J. Colloid Interface Sci.* **2004**, *280*, 334–342. [[CrossRef](#)]
23. Ko, D.; Mines, P.D.; Jakobsen, M.H.; Yavuz, C.T.; Hansen, H. Chr.B.; Andersen, H.R. Disulfide Polymer Grafted Porous Carbon Composites for Heavy Metal Removal from Stormwater Runoff. *Chem. Eng. J.* **2018**, *348*, 685–692. [[CrossRef](#)]
24. Vatankhah, H.; Riley, S.M.; Murray, C.; Quiñones, O.; Steirer, K.X.; Dickenson, E.R.V.; Bellona, C. Simultaneous Ozone and Granular Activated Carbon for Advanced Treatment of Micropollutants in Municipal Wastewater Effluent. *Chemosphere* **2019**, *234*, 845–854. [[CrossRef](#)]
25. Tang, L.; Ma, X.Y.; Wang, Y.; Zhang, S.; Zheng, K.; Wang, X.C.; Lin, Y. Removal of Trace Organic Pollutants (Pharmaceuticals and Pesticides) and Reduction of Biological Effects from Secondary Effluent by Typical Granular Activated Carbon. *Sci. Total Environ.* **2020**, *749*, 141611. [[CrossRef](#)]
26. Golea, D.M.; Jarvis, P.; Jefferson, B.; Moore, G.; Sutherland, S.; Parsons, S.A.; Judd, S.J. Influence of Granular Activated Carbon Media Properties on Natural Organic Matter and Disinfection By-Product Precursor Removal from Drinking Water. *Water Res.* **2020**, *174*, 115613. [[CrossRef](#)]
27. Belkouteb, N.; Franke, V.; McCleaf, P.; Köhler, S.; Ahrens, L. Removal of Per- and Polyfluoroalkyl Substances (PFASs) in a Full-Scale Drinking Water Treatment Plant: Long-Term Performance of Granular Activated Carbon (GAC) and Influence of Flow-Rate. *Water Res.* **2020**, *182*, 115913. [[CrossRef](#)]
28. Zhu, P.; Knoop, O.; Helmreich, B. Interaction of Heavy Metals and Biocide/Herbicide from Stormwater Runoff of Buildings with Dissolved Organic Matter. *Sci. Total Environ.* **2022**, *814*, 152599. [[CrossRef](#)] [[PubMed](#)]
29. Rommel, S.H.; Ebert, V.; Huber, M.; Drewes, J.E.; Helmreich, B. Spatial Distribution of Zinc in the Topsoil of Four Vegetated Infiltration Swales Treating Zinc Roof Runoff. *Sci. Total Environ.* **2019**, *672*, 806–814. [[CrossRef](#)] [[PubMed](#)]
30. Ouellet, V.; Khamis, K.; Croghan, D.; Hernandez Gonzalez, L.M.; Rivera, V.A.; Phillips, C.B.; Packman, A.I.; Miller, W.M.; Hawke, R.G.; Hannah, D.M.; et al. Green Roof Vegetation Management Alters Potential for Water Quality and Temperature Mitigation. *Ecohydrology* **2021**, *14*, e2321. [[CrossRef](#)]
31. Urbanczyk, M.M.; Bester, K.; Borho, N.; Schoknecht, U.; Bollmann, U.E. Influence of Pigments on Phototransformation of Biocides in Paints. *J. Hazard. Mater.* **2019**, *364*, 125–133. [[CrossRef](#)] [[PubMed](#)]
32. Paijens, C.; Bressy, A.; Frère, B.; Tedoldi, D.; Mailler, R.; Rocher, V.; Neveu, P.; Moilleron, R. Urban Pathways of Biocides towards Surface Waters during Dry and Wet Weathers: Assessment at the Paris Conurbation Scale. *J. Hazard. Mater.* **2021**, *402*, 123765. [[CrossRef](#)]
33. Schoknecht, U.; Mathies, H.; Lisec, J. Leaching and Transformation of Film Preservatives in Paints Induced by Combined Exposure to Ultraviolet Radiation and Water Contact under Controlled Laboratory Conditions. *Water* **2021**, *13*, 2390. [[CrossRef](#)]
34. Wang, J.; Guo, X. Adsorption Isotherm Models: Classification, Physical Meaning, Application and Solving Method. *Chemosphere* **2020**, *258*, 127279. [[CrossRef](#)] [[PubMed](#)]
35. Kalaruban, M.; Loganathan, P.; Nguyen, T.V.; Nur, T.; Hasan Johir, M.A.; Nguyen, T.H.; Trinh, M.V.; Vigneswaran, S. Iron-Impregnated Granular Activated Carbon for Arsenic Removal: Application to Practical Column Filters. *J. Environ. Manag.* **2019**, *239*, 235–243. [[CrossRef](#)] [[PubMed](#)]
36. Cai, Q.Q.; Wu, M.Y.; Hu, L.M.; Lee, B.C.Y.; Ong, S.L.; Wang, P.; Hu, J.Y. Organics Removal and In-Situ Granule Activated Carbon Regeneration in FBR-Fenton/GAC Process for Reverse Osmosis Concentrate Treatment. *Water Res.* **2020**, *183*, 116119. [[CrossRef](#)] [[PubMed](#)]
37. Peñafiel, M.E.; Matesanz, J.M.; Vanegas, E.; Bermejo, D.; Mosteo, R.; Ormad, M.P. Comparative Adsorption of Ciprofloxacin on Sugarcane Bagasse from Ecuador and on Commercial Powdered Activated Carbon. *Sci. Total Environ.* **2021**, *750*, 141498. [[CrossRef](#)]
38. Solanki, A.; Boyer, T.H. Physical-Chemical Interactions between Pharmaceuticals and Biochar in Synthetic and Real Urine. *Chemosphere* **2019**, *218*, 818–826. [[CrossRef](#)]
39. Rezakazemi, M.; Zhang, Z. 2.29 Desulfurization Materials. In *Comprehensive Energy Systems*; Dincer, I., Ed.; Elsevier: Oxford, UK, 2018; pp. 944–979, ISBN 978-0-12-814925-6.
40. Lesmana, S.O.; Febriana, N.; Soetaredjo, F.E.; Sunarso, J.; Ismadji, S. Studies on Potential Applications of Biomass for the Separation of Heavy Metals from Water and Wastewater. *Biochem. Eng. J.* **2009**, *44*, 19–41. [[CrossRef](#)]
41. Schreiber, B.; Brinkmann, T.; Schmalz, V.; Worch, E. Adsorption of Dissolved Organic Matter onto Activated Carbon—The Influence of Temperature, Absorption Wavelength, and Molecular Size. *Water Res.* **2005**, *39*, 3449–3456. [[CrossRef](#)]
42. Shimabuku, K.K.; Kennedy, A.M.; Mulhern, R.E.; Summers, R.S. Evaluating Activated Carbon Adsorption of Dissolved Organic Matter and Micropollutants Using Fluorescence Spectroscopy. *Environ. Sci. Technol.* **2017**, *51*, 2676–2684. [[CrossRef](#)]
43. Zhao, Z.; Sun, W.; Ray, M.B. Adsorption Isotherms and Kinetics for the Removal of Algal Organic Matter by Granular Activated Carbon. *Sci. Total Environ.* **2022**, *806*, 150885. [[CrossRef](#)]
44. Sountharajah, D.P.; Loganathan, P.; Kandasamy, J.; Vigneswaran, S. Effects of Humic Acid and Suspended Solids on the Removal of Heavy Metals from Water by Adsorption onto Granular Activated Carbon. *Int. J. Environ. Res. Public Health* **2015**, *12*, 10475–10489. [[CrossRef](#)] [[PubMed](#)]
45. Jiang, S.; Huang, L.; Nguyen, T.A.H.; Ok, Y.S.; Rudolph, V.; Yang, H.; Zhang, D. Copper and Zinc Adsorption by Softwood and Hardwood Biochars under Elevated Sulphate-Induced Salinity and Acidic pH Conditions. *Chemosphere* **2016**, *142*, 64–71. [[CrossRef](#)] [[PubMed](#)]

46. Zhou, R.; Zhang, M.; Shao, S. Optimization of Target Biochar for the Adsorption of Target Heavy Metal Ion. *Sci. Rep.* **2022**, *12*, 13662. [[CrossRef](#)] [[PubMed](#)]
47. Cibati, A.; Foereid, B.; Bissessur, A.; Hapca, S. Assessment of Miscanthus × Giganteus Derived Biochar as Copper and Zinc Adsorbent: Study of the Effect of Pyrolysis Temperature, pH and Hydrogen Peroxide Modification. *J. Clean. Prod.* **2017**, *162*, 1285–1296. [[CrossRef](#)]
48. Kim, D.-W.; Wee, J.-H.; Yang, C.-M.; Yang, K.S. Efficient Removals of Hg and Cd in Aqueous Solution through NaOH-Modified Activated Carbon Fiber. *Chem. Eng. J.* **2020**, *392*, 123768. [[CrossRef](#)]
49. Baup, S.; Wolbert, D.; Laplanche, A. Importance of Surface Diffusivities in Pesticide Adsorption Kinetics onto Granular Versus Powdered Activated Carbon: Experimental Determination and Modeling. *Environ. Technol.* **2002**, *23*, 1107–1117. [[CrossRef](#)]
50. Peng, B.; Chen, L.; Que, C.; Yang, K.; Deng, F.; Deng, X.; Shi, G.; Xu, G.; Wu, M. Adsorption of Antibiotics on Graphene and Biochar in Aqueous Solutions Induced by π - π Interactions. *Sci. Rep.* **2016**, *6*, 31920. [[CrossRef](#)]
51. Apul, O.G.; Wang, Q.; Zhou, Y.; Karanfil, T. Adsorption of Aromatic Organic Contaminants by Graphene Nanosheets: Comparison with Carbon Nanotubes and Activated Carbon. *Water Res.* **2013**, *47*, 1648–1654. [[CrossRef](#)]
52. Bhadra, B.N.; Seo, P.W.; Jhung, S.H. Adsorption of Diclofenac Sodium from Water Using Oxidized Activated Carbon. *Chem. Eng. J.* **2016**, *301*, 27–34. [[CrossRef](#)]
53. Xiaozhen, F.; Xing, L.; Zhenglin, H.; Kaiyuan, Z.; Guosheng, S. DFT Study of Common Anions Adsorption at Graphene Surface Due to Anion- π Interaction. *J. Mol. Model.* **2022**, *28*, 225. [[CrossRef](#)]
54. Al Bahri, M.; Calvo, L.; Gilarranz, M.A.; Rodriguez, J.J. Diuron Multilayer Adsorption on Activated Carbon from CO₂ Activation of Grape Seeds. *Chem. Eng. Commun.* **2016**, *203*, 103–113. [[CrossRef](#)]
55. de Souza, F.M.; dos Santos, O.A.A. Adsorption of Diuron from Aqueous Solution onto Commercial Organophilic Clay: Kinetic, Equilibrium and Thermodynamic Study. *Environ. Technol.* **2020**, *41*, 603–616. [[CrossRef](#)] [[PubMed](#)]
56. McGinley, J.; Healy, M.G.; Ryan, P.C.; Mellander, P.-E.; Morrison, L.; O'Driscoll, J.H.; Siggins, A. Batch Adsorption of Herbicides from Aqueous Solution onto Diverse Reusable Materials and Granulated Activated Carbon. *J. Environ. Manag.* **2022**, *323*, 116102. [[CrossRef](#)]
57. Huang, M.; Li, Z.; Huang, B.; Luo, N.; Zhang, Q.; Zhai, X.; Zeng, G. Investigating Binding Characteristics of Cadmium and Copper to DOM Derived from Compost and Rice Straw Using EEM-PARAFAC Combined with Two-Dimensional FTIR Correlation Analyses. *J. Hazard. Mater.* **2018**, *344*, 539–548. [[CrossRef](#)]
58. Genç-Fuhrman, H.; Mikkelsen, P.S.; Ledin, A. Simultaneous Removal of As, Cd, Cr, Cu, Ni and Zn from Stormwater Using High-Efficiency Industrial Sorbents: Effect of PH, Contact Time and Humic Acid. *Sci. Total Environ.* **2016**, *566*, 76–85. [[CrossRef](#)]
59. Esfandiari, N.; Suri, R.; McKenzie, E.R. Competitive Sorption of Cd, Cr, Cu, Ni, Pb and Zn from Stormwater Runoff by Five Low-Cost Sorbents; Effects of Co-Contaminants, Humic Acid, Salinity and pH. *J. Hazard. Mater.* **2022**, *423*, 126938. [[CrossRef](#)]
60. Zheng, X.; Yu, N.; Wang, X.; Wang, Y.; Wang, L.; Li, X.; Hu, X. Adsorption Properties of Granular Activated Carbon-Supported Titanium Dioxide Particles for Dyes and Copper Ions. *Sci. Rep.* **2018**, *8*, 6463. [[CrossRef](#)]
61. Eeshwarasinghe, D.; Loganathan, P.; Vigneswaran, S. Simultaneous Removal of Polycyclic Aromatic Hydrocarbons and Heavy Metals from Water Using Granular Activated Carbon. *Chemosphere* **2019**, *223*, 616–627. [[CrossRef](#)]
62. Wei, X.; Wu, Z.; Wu, Z.; Ye, B.-C. Adsorption Behaviors of Atrazine and Cr(III) onto Different Activated Carbons in Single and Co-Solute Systems. *Powder Technol.* **2018**, *329*, 207–216. [[CrossRef](#)]
63. Radian, A.; Mishaal, Y. Effect of Humic Acid on Pyrene Removal from Water by Polycation-Clay Mineral Composites and Activated Carbon. *Environ. Sci. Technol.* **2012**, *46*, 6228–6235. [[CrossRef](#)]
64. Lin, L.; Jiang, W.; Xu, P. Comparative Study on Pharmaceuticals Adsorption in Reclaimed Water Desalination Concentrate Using Biochar: Impact of Salts and Organic Matter. *Sci. Total Environ.* **2017**, *601*, 857–864. [[CrossRef](#)] [[PubMed](#)]
65. Jin, J.; Feng, T.; Gao, R.; Ma, Y.; Wang, W.; Zhou, Q.; Li, A. Ultrahigh Selective Adsorption of Zwitterionic PPCPs Both in the Absence and Presence of Humic Acid: Performance and Mechanism. *J. Hazard. Mater.* **2018**, *348*, 117–124. [[CrossRef](#)] [[PubMed](#)]

Disclaimer/Publisher's Note: The statements, opinions and data contained in all publications are solely those of the individual author(s) and contributor(s) and not of MDPI and/or the editor(s). MDPI and/or the editor(s) disclaim responsibility for any injury to people or property resulting from any ideas, methods, instructions or products referred to in the content.